RSC Advances

RSC Publishing

PAPER

Colorimetric sensing of copper(II) based on catalytic etching of gold nanorods

Cite this: *RSC Advances*, 2013, **3**, 13318

Zhaopeng Chen,*[a] Ruili Liu,[b] Shasha Wang,[ac] Chengli Qu,[a] Lingxin Chen[a] and Zhuo Wang[b]

Received 31st January 2013,
Accepted 13th May 2013

DOI: 10.1039/c3ra40559a

www.rsc.org/advances

In this work, a sensitive colorimetric method for determination of copper(II) in aqueous solution was developed based on catalytic etching of gold nanorods (GNRs). CTAB stabilized GNRs were etched slowly by dissolved oxygen along the axial direction in NH_3–NH_4Cl (0.8/0.1 M) solution. The etching was accelerated by the addition of Cu^{2+} with very low concentration, leading to a dramatic decrease of the GNRs in length but little in diameter. The etching caused the longitudinal surface plasmon resonance (LSPR) absorption to decrease sharply and shift to the short-wave direction, accompanied by a color change from blue to slight red. Potential effects of relevant experimental conditions, including concentrations of NH_3 and $S_2O_3^{2-}$, and incubation temperature and time were evaluated for optimization of the method. The proposed method is sensitive (LOD = 2.7 nM) and selective (by at least 100-fold over other metal ions except for Mn^{2+} and Pb^{2+}) with a linear range from 7 to 50 nM. Furthermore, the cost-effective method allows rapid and simple determination of the content of copper in shellfish samples.

Introduction

Copper is physiologically essential in various aspects such as cellular respiration, neurotransmitter biosynthesis, pigment formation, and connective tissue development. Copper is also a cofactor for numerous enzymes and plays an important role in central nervous system development. The deficiency of copper can lead to anemia or pancytopenia. However, Excess amounts of copper can result in emotional problems, behavioral disorders, mood swings, anemia, depression, kidney damage, eczema, schizophrenia, sickle-cell anemia, and central nervous system damage. The safe limit of copper in drinking water is 1.3 ppm ($\sim$20 μM) as recommended by the U.S. Environmental Protection Agency (EPA).[1] Therefore the detection of copper has attracted continuous attention in recent years. Many current techniques for the detection of Cu^{2+} ions, such as inductively coupled plasma mass spectrometry (ICP-MS),[2] atomic absorption/emission spectroscopy,[3] and atomic fluorescence spectrometry,[4] require expensive instruments and/or complicated sample preparation processes. UV spectrophotometry,[5] the evanescent wave infrared absorption spectroscopic method,[6] and anodic or cathodic stripping voltammetry[7] are either inconvenient for on-site monitoring, lack selectivity, or multi-step. Therefore, the development of inexpensive, reliable, and portable methods for copper(II) detection becomes more urgent. As an easily operated method, colorimetric method has proven to be practical in the determination of copper in natural waters and foods.[8] The major disadvantage of these methods is the relatively higher detection limits resulting from low photoabsorption coefficients of the Cu–organic complexes.

Nanoparticles-based colorimetric assays have recently attracted growing attention due to their simplicity and sensitivity. As nano-materials that can be easily synthesized and functionalized, gold nanoparticles (AuNPs) have a high molar extinction coefficient and have often been used as base materials for the colorimetric sensing of various targets,[9] *e.g.* proteins,[10] cells,[11] DNA[12] and metal ions.[13] The use of AuNPs as probes for the sensing of targets is usually based on the following two strategies. 1. Target induced AuNPs aggregation by formation of target-ligand complexes or by replacement of the stabilizer on AuNPs. This strategy suffers from complicated modifying processes or low sensitivity and selectivity. 2. Target etched/catalytically etched AuNPs which results in the decrease of the surface plasmon resonance absorption of AuNPs.[14] This strategy is a promising method for it possesses advantages such as label-free processes, sensitivity and selectivity. Unfortunately, few analytes can be determined by this method.

Here we developed a new colorimetric method using gold nanorods (GNRs) as a probe for the sensing of copper(II). Under ammonia medium, copper(II) catalytically etched the

[a]*Key Laboratory of Coastal Zone Environmental Processes and Ecological Remediation, Yantai Institute of Coastal Zone Research (YIC), Chinese Academy of Sciences (CAS); Shandong Provincial Key Laboratory of Coastal Zone Environmental Processes, YICCAS, Yantai, Shandong 264003, P. R. China.*
E-mail: zhpchen@yic.ac.cn
[b]*School of Environment and Materials Engineering, Yantai University, Yantai, Shandong 264003, P. R. China*
[c]*Graduate University of Chinese Academy of Sciences, Beijing 100049, China*

GNRs (the reaction is shown in eqn (1) and (2)),[15] resulting in a drastic decrease of the longitudinal surface plasmon resonance (LSPR) absorption of the GNRs. Compared with traditional methods and other AuNPs aggregation-based methods,[8,16] the probe shows more rapid (30 min), sensitive and feasible performance to naked eyes (the color change induced by 30 nM copper(II) can be easily observed).

$$Au + Cu(NH_3)_4^{2+} + S_2O_3^{2-} \rightarrow Au(S_2O_3)_2^{3-} + Cu(S_2O_3)_3^{5-} \quad (1)$$

$$Cu(S_2O_3)_3^{5-} + O_2 + NH_3 + 4H^+ \rightarrow Cu(NH_3)_4^{2+} + S_2O_3^{2-} \quad (2)$$

Experimental

Chemicals and apparatus

Hydrogen tetrachloroaurate(III) trihydrate, cetyltrimethylammonium bromide (CTAB), sodium thiosulfate ($Na_2S_2O_3$), $NaBH_4$, $AgNO_3$, ascorbic acid and all other chemicals used (analytical reagent grade or better) were obtained from Sinopharm Chemical Reagent (China). Deionized water (18.2 MΩ, Pall® Cascada) was used for the preparation of all the solutions. Images of transmission electron microscopy (TEM) were obtained from a JEM-1230 electron microscope working at 100 kV (Japan). UV-Visible absorption spectra for GNRs were recorded on a Nanodrop 2000c spectrophotometer (Thermo Scientific, USA).

Synthesis of GNRs

CTAB-capped gold nanorods were synthesized according to a typical seed-mediated method reported elsewhere.[17] Briefly, 7.5 ml of CTAB solution (0.1 M) was mixed with 0.25 ml of $HAuCl_4$ (0.01 mM) upon stirring, where 0.60 ml of fresh, ice-cold $NaBH_4$ solution (0.01 M) was then added, inducing the change of solution color to brown. The obtained solution was stirred for another 2 min and then was kept at 26 °C for 2 h. Then, after mixing 0.3 ml of $AgNO_3$ solution (10 mM) and 0.6 ml of $HAuCl_4$ solution (50 mM) with 49.9 ml of 0.10 M CTAB water solution at room temperature, 0.48 ml ascorbic acid (0.1 M) was added with gentle stirring. Immediately, the growth solution changed the color from dark yellow to colorless. 0.1 ml of the seed solution was subsequently added to the growth solution at room temperature. The solution was then left undisturbed for 20 h and the resulting colloid of GNRs was stored for further use. A TEM image showed the aspect ratio of GNRs to be 2.3 : 1.

Sensing procedure

For Cu^{2+} sensing, 200 μl of GNRs was added to 800 μl of NH_3/NH_4Cl buffers (pH 10.4) containing different concentrations of Cu^{2+}, then 5.0 mM $Na_2S_2O_3$ was added to the solution and equilibrated at 75 °C for 30 min. The solution was put into ice water for ~1 min to stop the reaction before UV-vis absorption spectra were recorded.

Analysis of practical samples

Local shellfish samples were wet digested for analyses. Briefly, the tissues were washed with deionized water thoroughly. After that, the samples were subsequently freeze-dried and ground to powders for digestion according to the following procedure. Briefly, to 0.3 g of powder sample, 10 ml ultrapure HNO_3 was added and the mixtures were digested in a high pressure tank at 150 °C for ~6 h. The digestive solutions were further diluted to 50.0 ml for use. During the test, 5–10 μl of diluted samples, 5.0 μl NaS_2O_3 (0.1 M), and 200 μl GNRs were successively added to 785 μl NH_3–NH_4Cl buffers. The solutions were incubated at 75 °C for 30 min before recording the absorption spectra. The concentrations of Cu^{2+} were calculated by the calibration curve.

Results and discussion

Sensing strategy

As a potential replacement for cyanide, the ionic system of $S_2O_3^{2-}$–Cu^{2+} has been demonstrated for the leaching and recovery of gold.[18] Although gold can be oxidized by dissolved oxygen in the presence of $S_2O_3^{2-}$, the high activation energy (E_a = 27.99 kJ mol^{-1}) limits the leaching progress. The activation energy can be reduced to only 15.54 kJ mol^{-1} by the addition of Cu^{2+}. The whole reaction process can be described as the following: copper ions first react with NH_3 to form a $Cu(NH_3)_4^{2+}$ complex. Then the formed $Cu(NH_3)_4^{2+}$ complex oxidizes gold to produce $Au(S_2O_3)_2^{3-}$ in the presence of $S_2O_3^{2-}$. Meanwhile, $Cu(NH_3)_4^{2+}$ is reduced to $Cu(S_2O_3)_3^{5-}$ which is re-oxidized to $Cu(NH_3)_4^{2+}$ by dissolved oxygen at the same time. Thus a circle reaction is formed. As there is abundant oxygen in the solution, Cu^{2+} acts only as a catalyst and is not consumed during the whole process.

Scheme 1 outlines the sensing procedure. The solution of GNRs (length/diameter ratio about 2.3 : 1) appeared blue owing to the intense longitudinal surface plasmon resonance (SPR) absorption of GNRs around 700 nm. The addition of 5 mM $S_2O_3^{2-}$ to the colloidal solution caused a color change from blue to bluish green in ammonia medium, indicating that the GNRs were etched slowly by dissolved oxygen. The etching was further accelerated in the presence of Cu^{2+} owing to its catalytic action accompanied by a color change from bluish green to slight red.

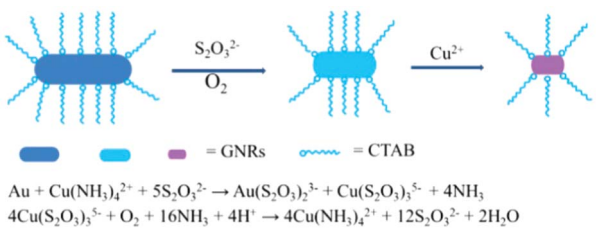

Scheme 1 Schematic illustration for the colorimetric sensing of Cu^{2+} based on the etching of GNRs.

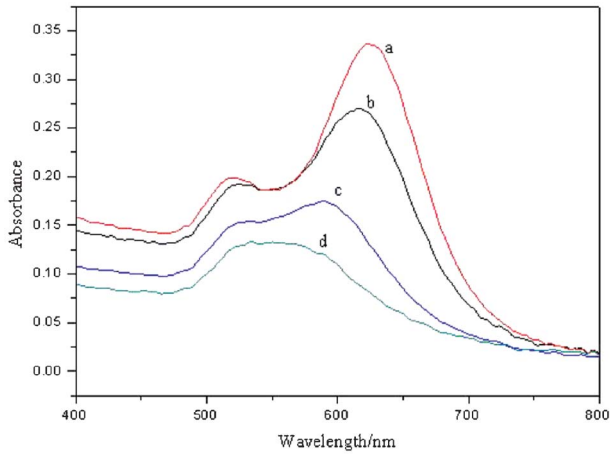

Fig. 1 The absorption spectra of GNRs after incubation with 5.0 mM $S_2O_3^{2-}$ with the absence of Cu^{2+} (a) and with the presence of 10 (b), 50 (c) and 100 nM Cu^{2+} (d). Other experimental conditions: buffer solution, NH_3/NH_4Cl (0.8/0.1 M); incubation temperature, 75 °C; incubation time, 30 min.

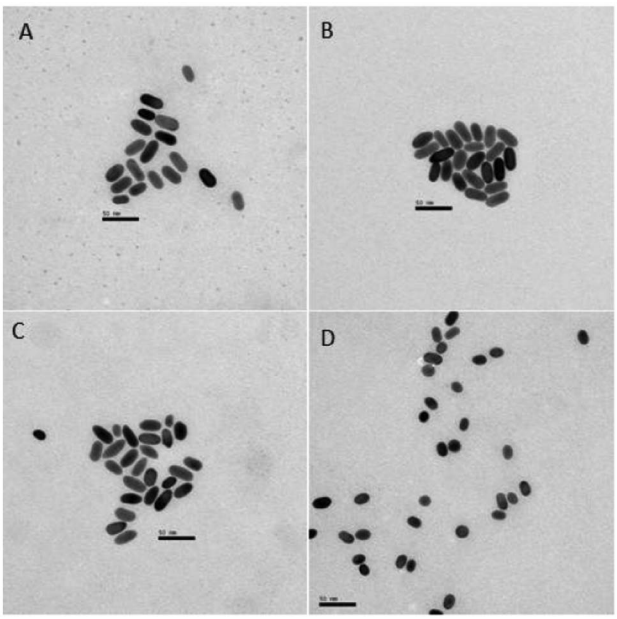

Fig. 2 TEM images of GNRs after incubation with 5.0 mM $S_2O_3^{2-}$ with the absence (A) and the presence of 10 (B), 50 (C) and 100 nM Cu^{2+} (D).

To confirm the etching of GNRs accelerated by Cu^{2+}, the absorption spectra of GNRs after incubation in ammonia medium containing 5 mM $S_2O_3^{2-}$ and different concentrations of Cu^{2+} were recorded. As shown in Fig. 1, the absorption spectrum of GNRs after incubation with 5 mM $S_2O_3^{2-}$ (curve a) exhibited strong SPR absorption at bands of 530 and 625 nm corresponding to the transverse and longitudinal SPR absorption, respectively. The absorption band at 625 nm gradually bleached and shifted to a shorter wavelength (curves b and c) with the further addition of different concentrations of Cu^{2+}. Our results, together with those of Zou[14c] and Stucky,[19] suggest that the blue-shift should be attributed to the decrease of aspect ratios (length/width) of GNRs and a preferential shortening along the axial direction. The preferential shortening along the axial direction can be attributed to less surface passivation and/or higher reaction activities at the tips of gold nanorods.[14c] The difference between TEM images before (Fig. 2A) and after (Fig. 2B, C and D) incubation of GNRs with Cu^{2+} also showed that the length/diameter ratio of GNRs decreased with the addition of Cu^{2+}, indicating that the etching of GNRs was accelerated by Cu^{2+}.

Optimization of experimental conditions

Since the method is based on accelerating the rate of gold leaching, the experimental conditions should be optimized to achieve high sensitivity. Factors to be tested include the concentrations of NH_3 and $S_2O_3^{2-}$, the incubation temperature and time. With respect to the fact that GNRs can also be etched by dissolved oxygen in the absence of Cu^{2+} with an obvious absorption decrease in longitudinal surface plasmon resonance (LSPR), the difference between the LSPR absorption of GNRs before and after addition of Cu^{2+} ($\Delta_A = A_{blank} - A_{sample}$) was chosen as a reference for optimization.

The effect of NH_3 on Δ_A was investigated in the absence and presence of Cu^{2+} (0.1 μM), while other factors were fixed (NH_4Cl = 0.1 M, $S_2O_3^{2-}$ = 5.0 mM, incubation T = 75 °C and time = 30 min). As shown in Fig. 3, in the absence of Cu^{2+}, the LSPR absorption kept stable with the increase of NH_3 from 0.2 to 0.8 M, and then decreased slightly. The slight decrease can be attributed to the increase of the conditional stability constant of $Au(S_2O_3)_2^{3-}$ with pH increasing and the consequent decrease of the practical redox potential of $Au(S_2O_3)_2^{3-}$/Au. While, in the presence of Cu^{2+}, the LSPR absorption decreased gradually with the increase of NH_3 from 0.2 to 0.6 M, since more $Cu(NH_3)_4^{2+}$ were formed in the solution. Further increase of NH_3 almost yielded no more effects. The Δ_A reached its maximum value when the concentration of NH_3 was set at 0.8 M. To achieve high sensitivity, the concentration of 0.8 M was selected in the following experiments.

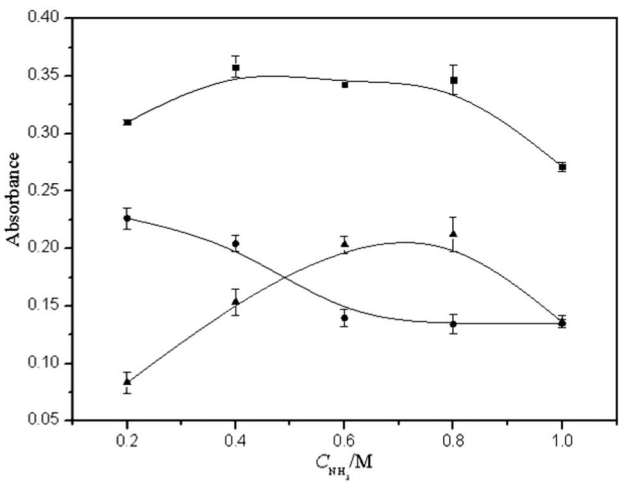

Fig. 3 LSPR absorbance of GNRs after incubation with 5.0 mM $S_2O_3^{2-}$ (■), 5.0 mM $S_2O_3^{2-}$ + 0.1 μM Cu^{2+} (●), and Δ_A (▲) in different concentrations of NH_3 at 70 °C for 30 min.

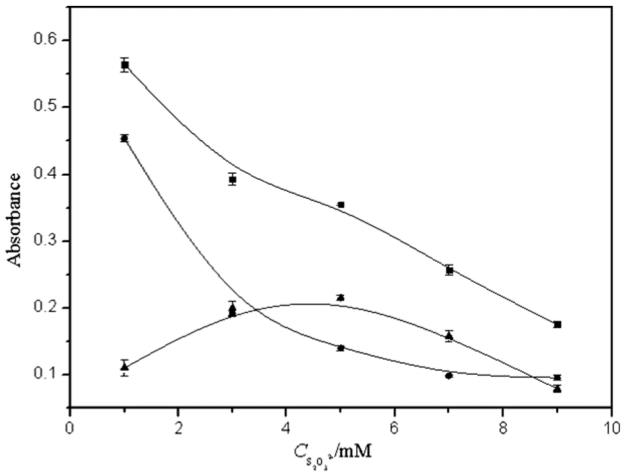

Fig. 4 LSPR absorbance of GNRs after incubation in NH_4Cl–NH_3 (0.1/0.8 M) buffer solution containing different concentrations of $S_2O_3^{2-}$ with the absence (■), and presence of 0.1 μM Cu^{2+} (●) and Δ_A (▲) at 75 °C for 30 min.

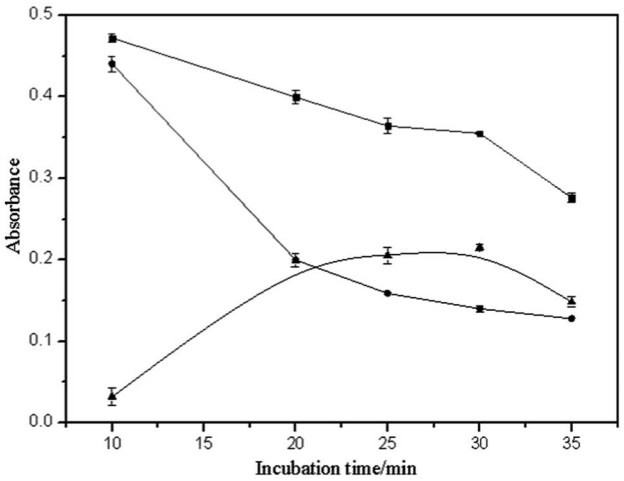

Fig. 6 LSPR absorbance of GNRs after incubation in NH_4Cl–NH_3 (0.1/0.6 M) buffer solution containing 5.0 mM $S_2O_3^{2-}$ with the absence (■), and presence of 0.1 μM Cu^{2+} (●) and Δ_A (▲) at 75 °C for different time.

The effect of $S_2O_3^{2-}$ on Δ_A was also investigated. As shown in Fig. 4, in the absence of Cu^{2+}, the LSPR absorption decreased linearly with the increase of $S_2O_3^{2-}$. The increasing $S_2O_3^{2-}$ decreased the practical redox potential and accelerated gold leaching. In the presence of Cu^{2+}, the LSPR absorption decreased sharply with the increase of $S_2O_3^{2-}$ from 1.0 to 5.0 mM. This should be attributed to both the decrease in the practical redox potential of $Au(S_2O_3)_2^{3-}$/Au and the increase in the redox potential of $Cu(NH_3)_4^{2-}$/$Cu(S_2O_3)_3^{5-}$. However, the effect was not remarkably promoted when $S_2O_3^{2-}$ exceeded 5.0 mM. The Δ_A reached its maximum value when the concentration of $S_2O_3^{2-}$ was set at 5.0 mM. As a result, $S_2O_3^{2-}$ with a concentration of 5.0 mM was chosen in following experiments.

Fig. 5 shows the effects of incubation temperature on Δ_A. Clearly, the LSPR absorption decreased linearly with the increase of incubation temperature in the absence of Cu^{2+}, while LSPR absorption decreased with the increase of the incubation temperature below 75 °C and then reached a plateau in the presence of Cu^{2+}. Additionally, the color change induced by Cu^{2+} was very sensitive to naked-eyes when the incubation temperature was set at 75 °C. As a result, an incubation temperature of 75 °C was thereby selected.

The effect of incubation time was shown in Fig. 6. The LSPR absorption decreased almost linearly with the increase of incubation time with the absence of Cu^{2+}. While in the presence of Cu^{2+}, the LSPR absorption decreased sharply with the increase of incubation time from 10 to 20 min and then reached a plateau. The Δ_A reached its maximum value when the incubation time was set at 30 min. The incubation time, 30 min, was selected.

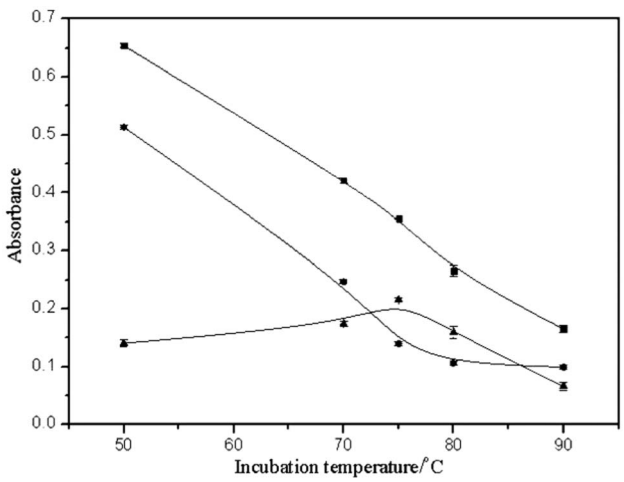

Fig. 5 LSPR absorbance of GNRs after incubation in NH_4Cl–NH_3 (0.1/0.6 M) buffer solution containing 5.0 mM $S_2O_3^{2-}$ with the absence (■), and presence of 0.1 μM Cu^{2+} (●) and Δ_A (▲) at different temperatures for 30 min.

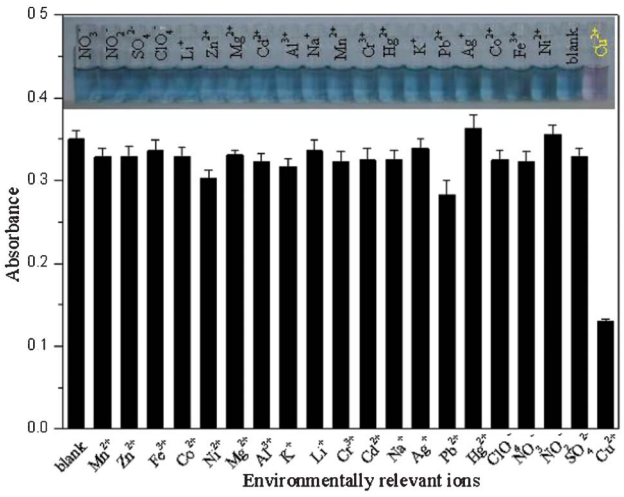

Fig. 7 LSPR absorbance of GNRs and the color of GNRs after incubation with common ions at 10 μM (except 0.1 μM Cu^{2+}, 0.1 μM Mn^{2+} and 1 μM Pb^{2+}) in NH_4Cl–NH_3 (0.1/0.8 M) buffer solution containing 5.0 mM $S_2O_3^{2-}$ at 75 °C for 30 min.

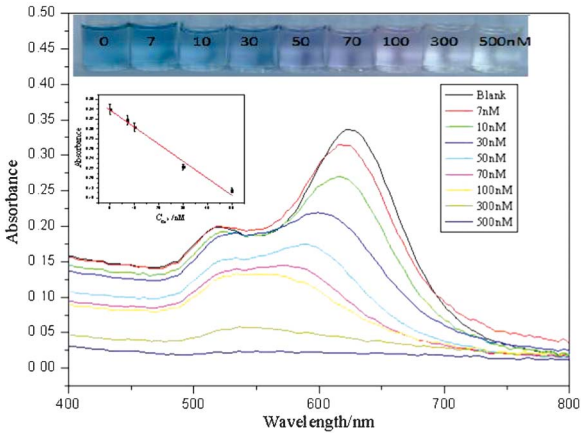

Fig. 8 LSPR absorbance and color change of GNRs after incubation with different concentrations of Cu^{2+} in NH_4Cl–NH_3 (0.1/0.8 M) buffer solution containing 5.0 mM $S_2O_3^{2-}$ at 75 °C for 30 min. Insets show the absorbance response to different concentrations of Cu^{2+} and the color change with the increase of Cu^{2+} concentration from left to right.

Table 1 Comparison of the quantitation results detected by ICP-MS and the proposed method

Samples	Found by ICP-MS/μM	Found by proposed probe/μM	Recoveries (%)
Sample 1	3.58	3.07	85.8
Sample 2	7.18	7.07	98.5
Sample 3	10.0	7.63	76.3
Sample 4	2.15	1.57	73.0

Selectivity of the sensor

To examine the selectivity of the developed sensor toward Cu^{2+}, Cu^{2+} and other common environmental ions were investigated under the optimum conditions. As shown in Fig. 7 it was obviously observed that the addition of 0.1 μM Cu^{2+} resulted in a dramatic LSPR decrease, while 100-fold of Ni^{2+}, Fe^{3+}, Co^{2+}, Ag^{+}, K^{+}, Hg^{2+}, Cr^{3+}, Na^{+}, Al^{3+}, Cd^{2+}, Mg^{2+}, Zn^{2+}, Li^{+}, ClO_4^{-}, SO_4^{2-}, NO_2^{-} and NO_3^{-}, 10-fold Pb^{2+} and the same concentration of Mn^{2+} almost did not cause any decrease of the LSPR. The digital photo (inset) also showed that only 0.1 μM Cu^{2+} caused an obvious color change of GNRs from green to slight red, while the color of GNRs was maintained as green in the presence of other environmental ions. Higher concentrations of Pb^{2+} showed a positive effect on gold etching due to the formation of Au–Pb alloy which decreased the redox potential of $Au(S_2O_3)_2^{3-}$/Au.[14a] As a result, the $S_2O_3^{2-}$–GNRs probe for Cu^{2+} provided excellent selectivity against other common environmental ions.

Sensitivity

To detect of the performance of the sensor, UV-vis spectra were employed to record the absorption of GNRs with various concentrations of Cu^{2+} ions under optimized conditions. Since the etching of GNRs caused a drastic decrease in LSPR absorption, we chose the Δ_A to plot the calibration curve against the concentration of Cu^{2+}. As shown in Fig. 8, with the increasing Cu^{2+}, the LSPR absorption decreased gradually. A linear range from 7.0 to 50.0 nM was obtained. The detection limit was calculated to be 2.7 nM (S/N = 3). The digital photo (inset) also showed that the color change induced by Cu^{2+} with a concentration more than 30 nM can be easily observed by naked-eyes, indicating the probe had a potential on-site application in the monitoring of Cu^{2+}.

Sample analysis

To evaluate the practicality for real samples, the proposed probe, was further applied to the sensing of Cu^{2+} in digested shellfish samples. The analytical results were consistent with those obtained by ICP-MS, indicating the method is applicable to the quantification of Cu^{2+} in shellfish samples. The applicability was also supported by similar comparative analyses of digested water samples (Table 1).

Conclusions

In summary, we developed a new rapid colorimetric assay for the sensitive and selective detection of Cu^{2+} based on the catalytic etching of GNRs with the aid of $S_2O_3^{2-}$. The intensity decrease in LSPR absorption and color change induced by

Table 2 Comparison of analytical performances of various typical techniques for copper analysis in aqeuous solution (1 μM = 64 ppb)

Method	Technique in detail	Linear range/detection limit	Selectivity	Ref.
ICP-OES	Solid phase extraction-ICP-OES detection	−/0.3 ppb	Good	20*a*
ICP-MS	Solid phase extraction-ICP-MS detection	−/39 ppt	Good	20*b*
Chromatography	Solid phase microextraction-high performance liquid chromatography	0.1–500 ppb/1 ppt	Good	20*c*
Voltammetry	Cysteine monolayers modified electrode-Osteryoung square wave voltammetry	0.05–5 ppb/0.025 ppb	Good	20*e*
Luminescence	16-mercaptohexadecanoic acid capped CdSe quantum dots	5–100 nM/5 nM	Good	20*f*
Fluorescence	branched poly(ethylenimine)-functionalized carbon quantum dots	10–1100 nM/6 nM	Good	20*g*
UV-vis spectrophotometry	Liquid–liquid microextraction-spectrophotometric detection	5–100 ppb/0.5 ppb	Not good	5
Colorimetry	Functionalized gold nanoparticles-copper catalyzed click chemistry	−/50 μM	Good	20*h*
Colorimetry	Copper inducing functionalized gold nanoparticles aggregation	0.05–25 μM/0.01 μM	Good	20*i*
Colorimetry	Catalytic leaching of silver-coated gold nanoparticles	5–800 nM/1.0 nM	Not good	20*j*
Colorimetry	Copper catalytic etching gold nanorods	7–50 nM/2.7 nM	Good	This work

Cu^{2+} provided a convenient way to monitor Cu^{2+}. The Cu^{2+}-specific probe exhibits high sensitivity towards Cu^{2+} and high selectivity over other environmental ions. Additionally, the method is also highlighted by its simplicity and rapidity compared to many conventional analytical methods, as well as other nanoparticles-based colorimetric methods (see in Table 2).[5,16,20] The color change induced by Cu^{2+} as low as 30 nM is remarkable enough to be observed by naked eyes which indicated that the proposed probe can be applied to field testing, avoiding the need of sophisticated equipment.

Acknowledgements

The research was financially supported by the Department of Science and Technology of Shandong Province (BS2009DX006), the Scientific Research Foundation for the Returned Overseas Chinese Scholars, State Education Ministry, the National Natural Science Foundation of China (21275158), the Innovation Projects of the Chinese Academy of Sciences (KZCX2-YW-JS208, KZCX2-EW-206), and the 100 Talents Program of the Chinese Academy of Sciences.

Notes and references

1 Y. T. Su, G. Y. Lan, W. Y. Chen and H. T. Chang, *Anal. Chem.*, 2010, **82**, 8566.
2 J. S. Becker, A. Matusch, C. Depboylu, J. Dobrowolska and M. V. Zoriy, *Anal. Chem.*, 2007, **79**, 6074.
3 (*a*) S. L. C. Ferreira, V. A. Lemos, B. C. Moreira, A. C. S. Costa and R. E. Santelli, *Anal. Chim. Acta*, 2000, **403**, 259; (*b*) G. P. C. Rao, K. Seshaiah, Y. K. Rao and M. C. Wang, *J. Agric. Food Chem.*, 2006, **54**, 2868.
4 L. He, X. Zhu, L. Wu and X. Hou, *Atom. Spectrosc.*, 2008, **29**, 93.
5 X. Wen, Q. Yang, Z. Yan and Q. Deng, *Microchem. J.*, 2011, **97**, 249.
6 G. G. Huang and J. Yang, *Anal. Chem.*, 2003, **75**, 2262.
7 (*a*) S. Legeai, S. Bois and O. Vittori, *J. Electroanal. Chem.*, 2006, **591**, 93; (*b*) P. Pathirathna, Y. Yang, K. Forzley, S. P. McElmurry and P. Hashemi, *Anal. Chem.*, 2012, **84**, 6298.
8 (*a*) B. K. Deshmukh, *Microchim. Acta*, 1983, **3**, 105; (*b*) O. Ozcan, M. Gultepe, O. M. Pcolu and E. Cakir, *Clin. Chem.*, 2006, **52**, A182.
9 (*a*) W. Zhao, M. A. Brook and Y. Li, *ChemBioChem*, 2008, **9**, 2363; (*b*) G. Wang, Y. Wang, L. Chen and J. Choo, *Biosens. Bioelectron.*, 2010, **25**, 1859.
10 (*a*) D. Aili, R. Selegard, L. Baltzer, K. Enander and B. Liedberg, *Small*, 2009, **5**, 2445; (*b*) Y. Xu, J. Wang, Y. Cao and G. Li, *Analyst*, 2011, **136**, 2044.
11 C. D. Medley, J. E. Smith, Z. Tang, Y. Wu, S. Bamrungsap and W. Tan, *Anal. Chem.*, 2008, **80**, 1067.
12 (*a*) M. S. Han, A. K. Lytton-Jean, B. K. Oh, J. Heo and C. A. Mirkin, *Angew. Chem., Int. Ed.*, 2006, **45**, 1807; (*b*) X. Zhu, Y. Li, J. Yang, Z. Liang and G. Li, *Biosens. Bioelectron.*, 2010, **25**, 2135.
13 H. Wei, B. Li, J. Li, S. Dong and E. Wang, *Nanotechnology*, 2008, **19**, 095501.
14 (*a*) Y.-Y. Chen, H.-T. Chang, Y.-C. Shiang, Y.-L. Hung, C.-K. Chiang and C.-C. Huang, *Anal. Chem.*, 2009, **81**, 9433; (*b*) L. Shang, L. Jin and S. Dong, *Chem. Commun.*, 2009, 3077; (*c*) R. Zou, X. Guo, J. Yang, D. Li, F. Peng, L. Zhang, H. Wang and H. Yu, *CrystEngComm*, 2009, **11**, 2797; (*d*) F.-M. Li, J.-M. Liu, X.-X. Wang, L.-P. Lin, W.-L. Cai, X. Lin, Y.-N. Zeng, Z.-M. Li and S.-Q. Lin, *Sens. Actuators, B*, 2011, **155**, 817; (*e*) Z. Chen, Z. Zhang, C. Qu, D. Pan and L. Chen, *Analyst*, 2012, **137**, 5197.
15 A. C. Grosse, G. W. Dicinoski, M. J. Shaw and P. R. Haddad, *Hydrometallurgy*, 2003, **69**, 1.
16 (*a*) C. Hua, W. H. Zhang, S. R. M. De Almeida, S. Ciampi, D. Gloria, G. Liu, J. B. Harper and J. J. Gooding, *Analyst*, 2012, **137**, 82; (*b*) Y.-F. Lee, T.-W. Deng, W.-J. Chiu, T.-Y. Wei, P. Roy and C.-C. Huang, *Analyst*, 2012, **137**, 1800; (*c*) S. K. Tripathy, J. Y. Woo and C.-S. Han, *Nanotechnology*, 2012, **23.**
17 T. K. Sau and C. J. Murphy, *Langmuir*, 2004, **20**, 6414.
18 G. Senanayake, *Miner. Eng.*, 2005, **18**, 995.
19 C. K. Tsung, X. S. Kou, Q. H. Shi, J. P. Zhang, M. H. Yeung, J. F. Wang and G. D. Stucky, *J. Am. Chem. Soc.*, 2006, **128**, 5352.
20 (*a*) D. Chen, B. Hu and C. Huang, *Talanta*, 2009, **78**, 491; (*b*) S. Chen, C. Liu, M. Yang, D. Lu, L. Zhu and Z. Wang, *J. Hazard. Mater.*, 2009, **170**, 247; (*c*) V. Kaur, J. S. Aulakh and A. K. Malik, *Anal. Chim. Acta*, 2007, **603**, 44; (*d*) Y. Guo, Z. Wang, W. Qu, H. Shao and X. Jiang, *Biosens. Bioelectron.*, 2011, **26**, 4064; (*e*) A. C. Liu, D. C. Chen, C. C. Lin, H. H. Chou and C. H. Chen, *Anal. Chem.*, 1999, **71**, 1549; (*f*) Y.-H. Chan, J. Chen, Q. Liu, S. E. Wark, D. H. Son and J. D. Batteas, *Anal. Chem.*, 2010, **82**, 3671; (*g*) Y. Dong, R. Wang, G. Li, C. Chen, Y. Chi and G. Chen, *Anal. Chem.*, 2012, **84**, 6220; (*h*) Y. Zhou, S. Wang, K. Zhang and X. Jiang, *Angew. Chem., Int. Ed.*, 2008, **47**, 7454; (*i*) S. Ye, X. Shi, W. Gu, Y. Zhang and Y. Xian, *Analyst*, 2012, **137**, 3365; (*j*) T. Lou, L. Chen, Z. Chen, Y. Wang, L. Chen and J. Li, *ACS Appl. Mater. Interfaces*, 2011, **3**, 4215.